

Coating effect on optical resonance of plasmonic nanobowtie antenna

Tzy-Rong Lin,^{1,2} Shu-Wei Chang,¹ Shun Lien Chuang,^{1,a)} Zhaoyu Zhang,^{3,4} and P. James Schuck³

¹Department of Electrical and Computer Engineering, University of Illinois at Urbana-Champaign, 1406 West Green Street, Urbana, Illinois 61801, USA

²Department of Mechanical and Mechatronic Engineering, National Taiwan Ocean University, Keelung 20224, Taiwan

³The Molecular Foundry, Lawrence Berkeley National Laboratory, Berkeley, California 94720, USA

⁴Department of Chemistry, University of California at Berkeley, Berkeley, California 94720, USA

(Received 30 April 2010; accepted 19 July 2010; published online 9 August 2010)

We investigate the effect of dielectric coating on the optical resonance of metallic bowtie nanoantennas, both theoretically and experimentally. The resonance wavelengths of the nanostructures measured by means of dark-field scattering spectroscopy are in excellent agreement with our theoretical calculations. The resonance wavelength is redshifted as the thickness of the coating layer increases, which is attributed to a longer effective optical path due to the larger refractive index of the coating than that of the air. © 2010 American Institute of Physics.

[doi:10.1063/1.3478228]

Metallic bowtie nanoantennas have been investigated theoretically and experimentally at optical wavelengths.^{1–5} The optical field between two metallic bowtie tips can be enhanced tremendously by the plasmonic resonance and curvature effect of bowtie tips. The enhanced optical field is confined in a volume which is only a small fraction of the cube of the resonance wavelength.⁶ Plasmonic resonance spectroscopy has been widely applied to biochemical sensing, biophotonics, and nanoscale devices.⁷ The strong field confinement provides a higher spatial resolution and more efficient excitation in the nanometer-scale regime, which are useful for a variety of applications, such as the surface enhanced Raman scattering,^{8,9} subwavelength optoelectronic devices,¹⁰ and near-field imaging.^{11,12} Surface plasmon polaritons exhibit a main field component normal to the metal-dielectric interface and an exponentially decreased profile toward both the metallic and dielectric regions away from the interface.¹³ Recently, the surface plasmon wave has been applied to plasmonic nanocavity lasers¹⁴ and plasmonic antenna lasers.^{6,15} Continuous-wave operation of metal-coated semiconductor lasers has also been demonstrated at room-temperature,^{16–18} which provides useful applications in addition to those of passive plasmonic devices.

In this paper, we report the effect of dielectric coating on the optical resonance of plasmonic bowtie nanoantennas in the experiment and use the finite-element method (FEM) to obtain the enhanced fields and resonance wavelengths for bowtie nanoantennas with different coating thicknesses, bowtie thicknesses, and tip-to-tip distances (gap widths). The dielectric coating provides the more flexible resonance tuning once a nanostructure is fabricated, and can be useful for the wavelength selectivity in many applications such as bio-sensing and chemical sensing. Our calculations confirm the large local field enhancement near the gold bowtie nanoantennas, which are fabricated on a silica substrate [covered with an indium-tin-oxide (ITO) layer] and coated with alumina (Al₂O₃). The resonance wavelengths from the FEM

calculations agree well with those from the experimental dark-field scattering spectra of bowtie nanoantennas. We show how the coating thickness, bowtie thickness, and gap width affect the resonance wavelengths.

Figure 1(a) shows the scanning electron microscopy (SEM) images of the fabricated gold bowtie nanoantennas and a designated coordinate system. The bowtie nanoantenna was then coated with an 8 nm alumina layer [Fig. 1(b)]. The geometry of the nanostructure in our calculation, which is very close to the fabricated bowtie, has a length of 75 nm, a thickness of 20 nm, a curvature radius of 10 nm at the tips, and an apex angle of 60°. The gap width between the two gold triangles of the bowtie is 25 nm. The substrate is fused silica with a 50 nm ITO layer. The origin of the coordinate system is placed at the center of the Au/ITO interface. In our calculations, the *x*-polarized electromagnetic wave incident along the positive *z* direction is used to excite the local field near the bowtie nanoantenna. This local field is then obtained based on the FEM from the commercial software COMSOL.¹⁹ The computation domain is enclosed by perfect-matched layers to avoid reflection. The refractive indices of gold, alumina, ITO, and silica are taken from Ref. 20.

Figure 2(a) shows the theoretical calculation of field enhancement ($|\mathbf{E}|^2/|\mathbf{E}_{x0}|^2$) on the horizontal plane which is 10 nm (half the bowtie thickness) above the Au/ITO interface. The surface plasmons significantly increase the field enhancement within the gap. For uncoated and coated structures, the maximum values (2043 and 1875) of field en-

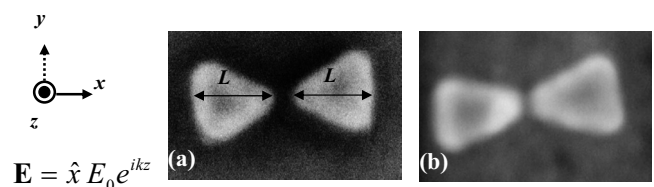


FIG. 1. The SEM images of (a) uncoated, and (b) Al₂O₃-coated gold bowties on the ITO/silica substrate. The length, *L*, of an equilateral-triangular bowtie is 75 nm. The bowtie nanoantennas are illuminated from the substrate along the positive *z* direction, and the incident electric field is *x*-polarized.

^{a)}Author to whom correspondence should be addressed. Electronic mail: s-chuang@illinois.edu.

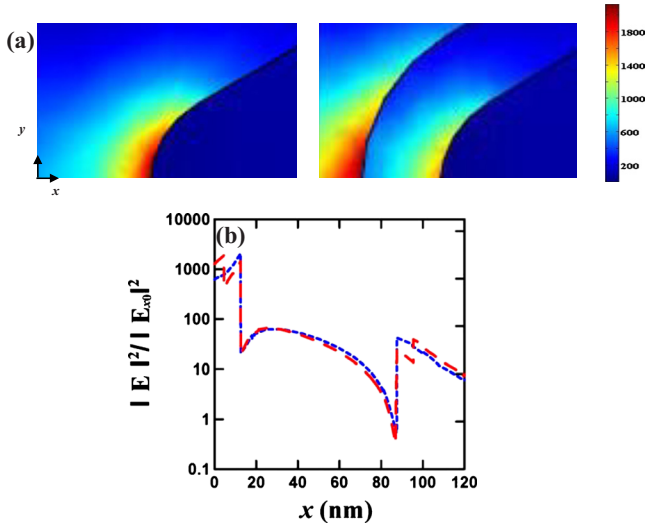


FIG. 2. (Color online) (a) Plots of the field enhancement $|E|^2/|E_{x0}|^2$ near the tips in the x - y plane at a height of one half of the bowtie thickness from the top of ITO layer without coating (left) and with an 8 nm Al_2O_3 coating (right). Both calculations are carried out at respective resonance wavelengths. (b) A logarithmic plot of $|E|^2/|E_{x0}|^2$ along the x direction for coated (long dashed) and uncoated (short dashed) antennas.

enhancements are found to be located at the bowtie tip ($x = 12.5$ nm, $y = 0$ nm) and the alumina-layer tip ($x = 4.5$ nm, $y = 0$ nm), respectively. The fields are small inside the gold bowtie. The plot of field enhancement along the x axis is also shown in Fig. 2(b). The x component of the electric fields is discontinuous at the air/gold interface (for no coating), as well as air/alumina and alumina/gold interfaces (for coating), to reflect the continuity of the x component of the electric displacement ($D_{x,i} = \epsilon_i E_{x,i}$, where i is the label of different regions) at the interfaces.²¹ The continuity (discontinuity) of the normal displacement (electric) field also indicates why the near field on the surface of a metallic nanostructure is usually enhanced significantly.

Figure 3 shows the experimental dark-field scattering spectra in the wavelength range 400–1000 nm for the bowtie nanoantennas shown in Fig. 1. From Fig. 3(a), a resonance peak at 710 nm is present on the spectrum of the bare bowtie (uncoated structure), and the counterpart of the coated bowtie in Fig. 3(b) shows a resonance wavelength at 790 nm. The alumina coating leads to the redshift of resonance wavelength. From the cavity perturbation, we can express the resonant frequency shift caused by material perturbation as²²

$$\frac{\omega - \omega_0}{\omega} = \frac{-\iiint_V dV [(\Delta\mu \cdot \mathbf{H}) \cdot \mathbf{H}^* + (\Delta\epsilon \cdot \mathbf{E}) \cdot \mathbf{E}^*]}{\iiint_V dV [\mu \mathbf{H} \cdot \mathbf{H}^* + \epsilon \mathbf{E} \cdot \mathbf{E}^*]} \quad (1)$$

Thus, the increase in permeability $\Delta\mu$ ($=0$ in this case) or permittivity $\Delta\epsilon$ of material inside the cavity decreases the resonance frequency. This wavelength redshift can also be explained via the wave number $k = 2\pi n_0/\lambda_0 \approx 2\pi n/\lambda$, where n_0 and n are the refractive indices of air and alumina coating, and λ_0 and λ are the resonance wavelengths of the uncoated structure and coated structure, respectively. The wave number reflects the spatial variation in the bowtie gap qualitatively. The alumina coating has a higher index than unity so that the extra index requires a longer wavelength to keep the wave number unchanged. In other words, the redshift is caused by a longer effective optical path due to the larger refractive index of the alumina coating than that of the air.

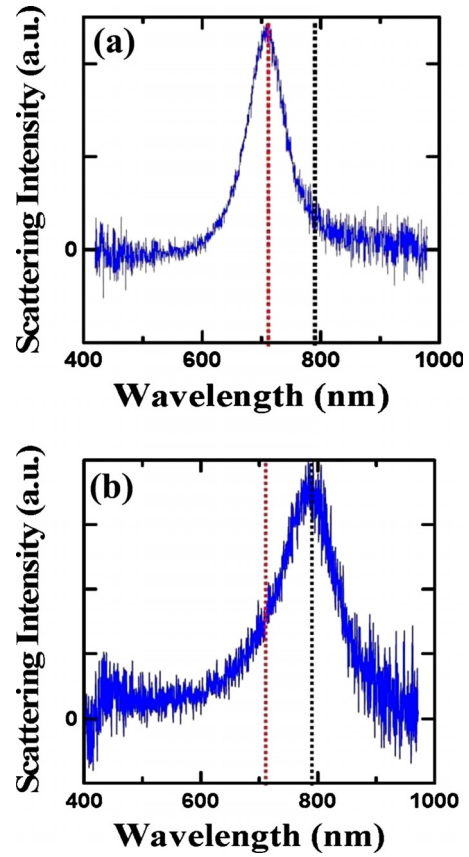


FIG. 3. (Color online) Experimental data of dark-field scattering spectra for the fabricated bowtie nanoantennas: (a) uncoated, and (b) with an 8 nm coating layer. The resonance wavelengths of the bare and coated bowties are 710 nm and 790 nm, respectively.

The calculated resonance spectra of the field enhancement for different coating thicknesses ($t = 0, 4,$ and 8 nm) are shown in Fig. 4. The observation point A is located at the center of the gap (10 nm above the Au/ITO interface). In Fig. 4, each resonance spectrum has one resonance peak (resonance wavelength $\lambda_{\text{res}} = 714, 754,$ and 781 nm for $t = 0, 4,$ and 8 nm, respectively). The resonance wavelength and corresponding redshift at $t = 8$ nm from the FEM calculation are in excellent agreement with the experimental data. More-

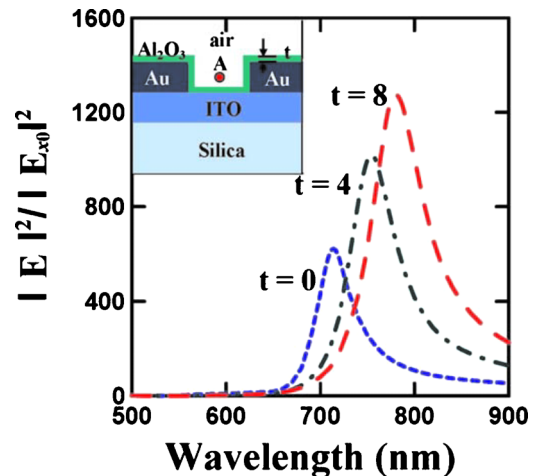


FIG. 4. (Color online) Theoretical calculations of the field enhancement $|E|^2/|E_{x0}|^2$ vs wavelength for different coating thicknesses $t = 8$ nm (long dashed), 4 nm (dashed-dotted), and 0 nm (short dashed). The inset shows a schematic drawing of the coated bowtie nanoantennas.

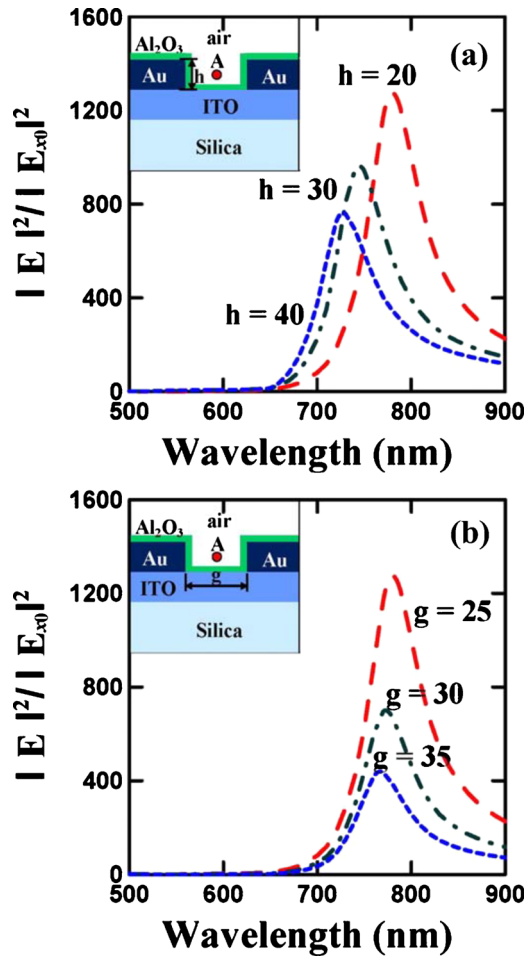


FIG. 5. (Color online) Theoretical calculations of electric field enhancement vs wavelength for bowtie nanoantennas with (a) a 25 nm gap and three different bowtie thicknesses $h=20$ nm (long dashed), 30 nm (dashed-dotted), and 40 nm (short dashed); (b) a 20 nm bowtie thickness and three different gap widths: $g=25$ nm (long dashed), 30 nm (dashed-dotted), and 35 nm (short dashed). The observation point A is located at the center of the gap and a height of one half of the bowtie thickness.

over, we find that the amounts of redshift and field enhancement increase as the coating thickness increases. The increasing field enhancement is mainly due to an observation point closer to the alumina-coated tip as the coating thickness increases. However, the maximum field enhancement is still located at the tip, as shown in Fig. 2.

Figure 5 shows the resonance spectra of field enhancement from the FEM calculations under different bowtie thicknesses h and different gap widths g . If the bowtie thickness or gap width is small, as indicated by the curve for $h=20$ nm in Fig. 5(a) or that for $g=25$ nm in Fig. 5(b), the spectrum shows a large field enhancement. In addition, accompanied by the increase in field enhancement as the bowtie thickness h or gap width g decreases, the resonance wavelength also exhibits a redshift, as indicated in Fig. 5. Such a tendency is similar to that of a pair of spherical particles.²³ The increase in the field enhancement as h decreases has a similar origin to that as the coating thicknesses t becomes larger. In this case, a smaller h means that the point A is closer to the bottom $\text{Al}_2\text{O}_3/\text{air}$ interface, where the field is maximal due to the nature of surface wave. On the other hand, the increase in the field enhancement as g decreases is caused by the more localized field distribution. As

g decreases, the field at the point A becomes larger because the exponential decay of the surface wave into the air region is incomplete. This phenomenon is analogous to that of a metal-dielectric-metal plasmonic slab waveguide—the more significant field confinement occurs when the dielectric region becomes narrower.

In summary, we have studied the optical resonance of gold bowtie nanoantennas coated with an alumina layer. The theoretical calculations are compared with the experimental data from the dark-field scattering spectroscopy, and the calculated resonance wavelengths are in excellent agreement with experiment. When the thickness of the coating layer increases, the resonance wavelength exhibits a redshift. From our theoretical results, redshifts also occur when the bowtie thickness or the gap width decreases. In all three cases, we obtain significant field enhancements, which are accompanied by a redshift of the resonance wavelengths.

This work was sponsored by the DARPA NACHOS Program under Grant No. W911NF-07-1-0314. We thank many technical discussions with Professors Connie Chang-Hasnain, Ming Wu, and Peidong Yang at the University of California at Berkeley, Professor Cun-Zheng Ning at Arizona State University, and Chien-Yao Lu and Chi-Yu Ni at the University of Illinois at Urbana-Champaign.

- ¹N. Yu, E. Cubukcu, L. Diehl, D. Bour, S. Corzine, J. Zhu, G. Höfler, K. B. Crozier, and F. Capasso, *Opt. Express* **15**, 13272 (2007).
- ²Z. Rao, L. Hesselink, and J. S. Harris, *Opt. Lett.* **32**, 1995 (2007).
- ³E. X. Jin and X. Xu, *Appl. Phys. Lett.* **88**, 153110 (2006).
- ⁴D. P. Fromm, A. Sundaramurthy, P. J. Schuck, G. Kino, and W. E. Moerner, *Nano Lett.* **4**, 957 (2004).
- ⁵D. A. Genov, A. K. Sarychev, V. M. Shalaev, and A. Wei, *Nano Lett.* **4**, 153 (2004).
- ⁶S. W. Chang, C. Y. Ni, and S. L. Chuang, *Opt. Express* **16**, 10580 (2008).
- ⁷Y. Cao, R. Jin, and C. A. Mirkin, *Science* **297**, 1536 (2002).
- ⁸P. P. Pompa, L. Martiradonna, T. A. Della, S. F. Della, L. Manna, M. V. De, F. Calabi, R. Cingolani, and R. Rinaldi, *Nat. Nanotechnol.* **1**, 126 (2006).
- ⁹A. Weber-Bargioni, A. Schwartzberg, M. Schmidt, B. Harteneck, D. F. Ogletree, P. J. Schuck, and S. Cabrini, *Nanotechnology* **21**, 065306 (2010).
- ¹⁰S. A. Maier, P. G. Kik, and H. A. Atwater, *Appl. Phys. Lett.* **81**, 1714 (2002).
- ¹¹S. Takahashi and A. V. Zayats, *Appl. Phys. Lett.* **80**, 3479 (2002).
- ¹²Z. Zhang, A. Weber-Bargioni, S. W. Wu, S. Dhuey, S. Cabrini, and P. J. Schuck, *Nano Lett.* **9**, 4505 (2009).
- ¹³W. L. Barnes, A. Dereux, and T. W. Ebbesen, *Nature (London)* **424**, 824 (2003).
- ¹⁴M. T. Hill, Y. S. Oei, B. Smalbrugge, Y. Zhu, T. D. Veries, P. J. Ven Veldhoven, F. W. M. Van Otten, T. J. Eijkemans, J. P. Turkwieicz, H. De Waardt, E. J. Geluk, S. H. Kwon, Y. H. Lee, R. Nötzel, and M. K. Smit, *Nat. Photonics* **1**, 589 (2007).
- ¹⁵N. Yu, E. Cubukcu, L. Diehl, M. A. Belkin, K. B. Crozier, F. Capasso, D. Bour, S. Corzine, and G. Höfler, *Appl. Phys. Lett.* **91**, 173113 (2007).
- ¹⁶C. Y. Lu, S. W. Chang, S. H. Yang, and S. L. Chuang, *Appl. Phys. Lett.* **95**, 233507 (2009).
- ¹⁷G. E. Chang, C. Y. Lu, S. H. Yang, and S. L. Chuang, *Opt. Lett.* **35**, 2373 (2010).
- ¹⁸C. Y. Lu, S. W. Chang, S. L. Chuang, T. D. Germann, and D. Bimberg, *Appl. Phys. Lett.* **96**, 251101 (2010).
- ¹⁹COMSOL MULTIPHYSICS, Comsol Inc. (<http://www.comsol.com>).
- ²⁰E. D. Palik, *Handbook of Optical Constants of Solids* (Academic, New York, 1998).
- ²¹S. A. Maier, *Plasmonics: Fundamentals and Applications* (Springer, New York, 2007).
- ²²J. A. Kong, *Electromagnetic Wave Theory* (EMW, Cambridge, 2008).
- ²³H. Tamaru, H. Kuwata, H. T. Miyazaki, and K. Miyano, *Appl. Phys. Lett.* **80**, 1826 (2002).